Correlation between Point Mutations in NS2 and the Viability and Cytopathogenicity of Bovine Viral Diarrhea Virus Strain Oregon Analyzed with an Infectious cDNA Clone

BEATE M. KÜMMERER† AND GREGOR MEYERS*

Federal Research Centre for Virus Diseases of Animals, D-72076 Tübingen, Germany

Cytopathogenicity of *Bovine viral diarrhea virus* (BVDV) is correlated with expression of the nonstructural protein NS3, which can be generated by processing of a fusion protein termed NS2-3. For the cytopathogenic (cp) BVDV strain Oregon, NS2-3 processing is based on a set of point mutations within NS2. To analyze the correlation between NS2-3 cleavage and cytopathogenicity, a full-length cDNA clone composed of cDNA from BVDV Oregon and the utmost 5′- and 3′-terminal sequences of a published infectious BVDV clone was established. After transfection of RNA transcribed from this cDNA clone, infectious virus with similar growth characteristics to wild-type BVDV Oregon could be recovered that also exhibited a cytopathic effect. Based on this cDNA construct and published cp and noncp infectious clones, chimeric full-length cDNA clones were constructed. Analysis of the recovered viruses demonstrated that the presence of the NS2 gene of BVDV Oregon in a chimeric construct is sufficient for NS2-3 processing and a cp phenotype. Since previous studies had revealed that the amino acid serine at position 1555 of BVDV Oregon plays an important role in efficient NS2-3 cleavage, mutants of BVDV Oregon with different amino acids at this position were constructed. Some of these mutants showed NS2-3 cleavage efficiencies in the range of the wild-type sequence and allowed the recovery of viruses that behaved similarly to wild-type virus with regard to growth characteristics and cytopathogenicity. In contrast, other mutants with considerably reduced NS2-3 cleavage efficiencies propagated much more slowly and reverted to viruses expressing polyproteins with sequences allowing efficient NS2-3 cleavage. These viruses apparently induced cytopathic effects only after reversion.

Bovine viral diarrhea virus (BVDV) belongs to the genus *Pestivirus* within the family *Flaviviridae*. This virus family also contains the genus *Flavivirus* and the hepatitis C-like viruses (41). The other members of the genus *Pestivirus* are *Classical swine fever virus* (CSFV) and *Border disease virus* of sheep. The genome of these viruses consists of a single-stranded RNA of positive polarity, usually having a length of 12.3 kb (26). The RNA possesses one long open reading frame that encodes a polyprotein of about 4,000 amino acids (26). The latter is processed co- and posttranslationally by host cell and viral proteases to give rise to the mature virus proteins. N^{pro}, the protein at the N terminus of the polyprotein, represents a nonstructural protein with autoproteolytic activity (30, 34). It is followed by the structural proteins, i.e., the capsid protein C and the three glycoproteins E^{rns}, E1, and E2 (26). The C-terminal two-thirds of the polyprotein contains the remaining nonstructural proteins (NS) in the order p7, NS2, NS3, NS4A, NS4B, NS5A, and NS5B (26).

Pestiviruses represent important pathogens of animals. The most severe manifestation of a BVDV infection is the so-called mucosal disease (1, 37). Elaborate studies elucidated that two biotypes of BVDV, noncytopathogenic (noncp) and cytopathogenic (cp) viruses, are involved in the development of this lethal disease. In a first step, intrauterine infection in an early stage of gestation has to occur, and this induces a specific immunotolerance and results in the birth of a persistently infected calf (37). Such animals may come down with mucosal disease, which usually happens early in life. The induction of the disease is based on either superinfection with an antigenetically closely related cp BVDV or generation of a cp mutant of the persisting noncp virus (4, 6, 23, 37). Molecular analyses showed that most cp viruses develop from noncp viruses by RNA recombination (20). For these cases, the molecular events leading to a cp virus include insertion of cellular sequences, duplication and rearrangement of pestivirus sequences, and deletion of pestivirus sequences. These genome alterations lead to a characteristic feature of cp BVDV, namely, the expression of the nonstructural protein NS3 (20). NS3 represents the C-terminal part of NS2-3, which is found in cells infected with either cp viruses or noncp viruses.

Recently, we demonstrated a new mechanism for expression of the NS3 protein that is not due to RNA recombination. Instead, processing of NS2-3 is based on several point mutations within the nonstructural protein NS2 (16). These data were determined for BVDV Oregon and represented the first formal proof of the existence of a cp BVDV not generated by RNA recombination. However, there is good evidence that cytopathogenicity based on point mutations is not a unique feature of BVDV Oregon but is also true for some other cp isolates. For all these viruses, including BVDV Oregon, corresponding noncp isolates are missing. Thus, it is not possible to identify the relevant mutations directly by sequence comparison.

Because of the high error rate of RNA-dependent RNA polymerases, it can be assumed that accumulation of point mutations is more probable than occurrence of an RNA recombination that leads to a viable virus. However, the number of cp BVDV strains for which point mutations seem to be responsible for the generation of NS3 is apparently signifi-

* Corresponding author. Mailing address: Federal Research Centre for Virus Diseases of Animals, P.O. Box 1149, D-72001 Tübingen, Germany. Phone: 49 7071-967207. Fax: 49 7071-967303. E-mail: gregor .meyers@tue.bfav.de.

† Present address: Department of Molecular Microbiology, Washington University School of Medicine, St. Louis, MO 63110-1093.

cantly smaller than the number of those expressing NS3 due to changes resulting from RNA recombination (7, 13, 16, 20; G. Meyers, unpublished data). This suggests the existence of some kind of barrier preventing the generation of cp BVDV by point mutations. To be able to analyze this question in detail, we established an infectious cDNA clone for BVDV Oregon and investigated the correlation between individual point mutations, cytopathogenicity, and viability of BVDV Oregon mutants.

MATERIALS AND METHODS

Cells and viruses. MDBK cells were obtained from the American Type Culture Collection (Rockville, Md.). BHK-21 cells (BSR clone) were kindly provided by J. Cox (Federal Research Centre for Virus Diseases of Animals, Tübingen, Germany). Cells were grown in Dulbecco's modified Eagle's medium (DMEM) supplemented with 10% fetal calf serum (FCS) and nonessential amino acids. The cp BVDV strain Oregon (12) was kindly provided by B. Liess (University of Hanover, Hanover, Germany). The T7 vaccinia virus (vTF7-3) (11) was generously provided by B. Moss (Laboratory of Viral Diseases, National Institute of Allergy and Infectious Diseases, Bethesda, Md.).

Infection of cells. Since pestiviruses are mainly cell associated (14), lysates of infected cells were used for reinfection of culture cells. Material for infection was prepared by freezing and thawing cultures 48 h postinfection and stored at −70°C. If not specified, a multiplicity of infection (MOI) of 0.1 was used.

Virus immunofluorescence assay, virus peroxidase assay, and crystal violet staining. For immunofluorescence and peroxidase assays, cells were fixed with ice-cold methanol-acetone (1:1) for 15 min, air dried, rehydrated with phosphate-buffered saline (PBS), and then incubated for 1 h at 37°C with a mixture of monoclonal antibodies (MAb) directed against E2 (40). For the immunofluorescence assay, plates were washed three times with PBS and bound antibodies were detected with fluorescein isothiocyanate-conjugated goat anti-mouse serum (1 h at 37°C) (Dianova, Hamburg, Germany). For peroxidase staining, peroxidase-conjugated goat anti-mouse antibodies (Dianova) were used as second antibodies. After incubation for 1 h at room temperature, the supernatant was discarded and fixed cells were washed three times with PBS. Detection was performed with a solution composed of 0.5 ml of 1 M sodium acetate buffer (pH 5.0), 0.5 ml of aminoethylcarbazole solution (4 mg of aminoethylcarbazole per milliliter of dimethylformamide), 9.5 ml of H$_2$O, and 10 μl of H$_2$O$_2$. After incubation for 20 to 30 min at room temperature in the dark, excess substrate was removed and the plates were rinsed with water.

Crystal violet staining was performed after cells were washed once with PBS, fixed for 10 min with 5% formaldehyde, and washed again with water. For staining, the cells were incubated for 5 min with 1% (wt/vol) crystal violet in 50% ethanol.

Nucleotide sequencing. Sequencing of double-stranded DNA was carried out with the T7 polymerase sequencing kit (Pharmacia; Freiburg, Germany) (32). For direct sequencing of PCR fragments, about 1/10 of the PCR mixture was used after purification of the fragment by agarose gel electrophoresis and extraction with the QIAEX II gel extraction kit (Qiagen, Hilden, Germany). Sequence analysis and sequence alignments were done with Genetics Computer Group software (9).

RT-PCR and PCR. Total RNA from MDBK cells infected with BVDV Oregon was used as starting material for reverse transcription-PCR (RT-PCR). Heat denaturation of 2.5 μg of total cellular RNA (2 min at 92°C followed by 5 min on ice) was done in a total volume of 37 μl containing 15 μl of PCR mix (50 mM Tris-HCl [pH 8.3], 150 mM KCl, 5 mM MgCl$_2$, 0.5 mM deoxynucleoside triphosphates) and 30 pmol of reverse primer. Reverse transcription was done for 45 min at 37°C after adding 5 μl of PCR mix, 15 U of RNA guard (Pharmacia), and 50 U of reverse transcriptase (Superscript, Life Technologies/Bethesda Research Laboratories, Eggenstein, Germany). After addition of paraffin (Paraplast; melting point, 55°C) and heating for 2 min at 80°C, the tubes were placed on ice and 5 μl of PCR mix, 30 pmol of upstream primer, and 2.5 U of Taq polymerase (Appligene, Heidelberg, Germany) in a total volume of 7.5 μl were added. Amplification was carried out for 30 cycles (30 s at 94°C, 30 s at 54 to 56°C, and 30 to 120 s at 72°C). The oligonucleotides used for RT-PCR have the following sequences: BVDV 56 (positive orientation), GAGATCTCGGGAGGTAC; BVDV 57 (negative orientation), CCTCTCGGCATGATCCCGAAA.

Construction of full-length BVDV cDNA clones. Restriction, cloning, and other standard procedures were done essentially as described previously (31). Restriction and modifying enzymes were obtained from New England BioLabs (Schwalbach, Germany), Pharmacia, and Boehringer-Mannheim GmbH (Mannheim, Germany). To create blunt ends, the Klenow fragment of DNA polymerase I was used. Dephosphorylation was carried out with calf intestinal phosphatase. Nucleotide and amino acid positions refer to BVDV SD-1 (8).

pC7 was obtained after ligation of a PCR fragment (primers B53 and 3′ SrfI; template, pA/BVDV [22]) cut with AatII and XmaI, together with an XmaI-ApaLI fragment (the AatII site was deleted by cutting, treatment with Klenow, and religation) derived from pA/CSFV (21) and an ApaLI-AatII fragment derived from pA/BVDV.

Construction of the full-length cDNA clone of BVDV Oregon was based mainly on the cDNA clones pO1.37, pO1.18, pO1.13, and pO1.2 described previously (16). In addition, two fragments generated by RT-PCR were used. The PCR fragment used for construction of the 5′ part of the genome of BVDV Oregon was amplified with primers ORT37 and BL78. The PCR product was treated with Klenow, cut with SacI, and ligated into pBluescript SK(−)/SacI-EcoRV. For construction of the 3′ part of the genome, a fragment was amplified by RT-PCR (primers B50/BVD49), treated with Klenow, cut with BamHI, and inserted into pBluescript SK(−)/BamHI-EcoRV. The PCR fragments were checked by nucleotide sequencing and then used for further cloning. Details of the cloning procedures are available on request.

Clone pC7$_{NS2/C7Ins−}$ was generated by digesting pC7 with NsiI and AatII and inserting the NsiI-SacI fragment from expression construct pC7.1Ins− (35) together with the SacI-AatII fragment from pC7. For construction of pC7$_{NS2/OR}$, an EcoRI-HincII fragment from pC7, a HincII-BamHI fragment from pC7 which contained a silent XhoI site at positions 5126 to 5131 (16), and an XmaI-XhoI fragment from pO1* (16) were assembled into pCITE-2a/EcoRI-XhoI. From the resulting clone, an XhoI-NsiI (partially cut) fragment was released and was inserted together with an XhoI-AatII fragment, obtained from a derivative of pC7 that contained a silent XhoI site at positions 5126 to 5131, into pC7 cut with NsiI and AatII. To obtain pOR$_{NS2/C7Ins−}$, a SpeI-XmaI (silent) (16) fragment derived from the Oregon sequence was inserted together with an XmaI-SalI fragment from pO1-1 (16) into pBluescript SK(−) to give p245; thereafter, a Bsu36I-XhoI fragment was released from p245 and assembled together with an XhoI-AatII fragment of pOR/XhoI into pOR cut with Bsu36I and AatII. For construction of pOR$_{NS2/C7}$, a KpnI-SphI fragment from p245 was exchanged with the respective fragment from pC7; from the resulting clone, a Bsu36I-XhoI fragment was released and assembled with the fragments described for pOR$_{NS2/C7Ins−}$.

For construction of the derivatives of pOR containing exchanges at codon 1555 of the open reading frame, the ClaI-SalI fragment of pOR was exchanged with the respective fragment containing the desired mutation.

The oligonucleotides have the following sequences: B53 (positive orientation) GCCAGAGACAACTCCATC; 3′ Srf (negative orientation), TTCCCCCGGG CTGTTAAAGGTCTTCC; ORT37 (positive orientation), GTGAGTTCGTTG GATGG; BL78 (negative orientation), ACGTTTAGGTCACTATCCCT; B50 (positive orientation), CTAGTAGAGATCTACGGC; and BVD49 (negative orientation), GCACCCGGGGCTGTTA(G/A)(A/G)GGTCTTCCCTAG.

Site-directed mutagenesis. All mutants were generated by the method of Kunkel et al. (17) with the Muta-Gene Phagemid in vitro mutagenesis kit (Bio-Rad, Munich, Germany) essentially as described by the manufacturer, except that single strands were produced with the filamentous phage VCSM13 (Stratagene). Oligonucleotide primers specifying single- or double-base changes were used in the mutagenesis reactions. The mutations of codon 1555 leading to the respective amino acid exchanges are shown in Table 1. All of the subcloned fragments used for mutagenesis were sequenced to verify the presence of the desired mutations and the absence of second-site mutations.

In vitro transcription. A 2-μg portion of the respective cDNA construct was linearized with the appropriate restriction enzyme and purified by phenol extraction and ethanol precipitation. Transcription with T7 RNA polymerase (New England BioLabs) was carried out in a total volume of 50 μl of transcription mix (40 mM Tris-HCl [pH 7.5]; 6 mM MgCl$_2$; 2 mM spermidine; 10 mM NaCl; 0.5 mM each ATP, GTP, CTP, and UTP; 10 mM dithiothreitol; 100 μg of bovine serum albumin per ml) with 50 U of T7 RNA polymerase in the presence of 15 U of RNA guard (Pharmacia). After incubation at 37°C for 1 h, 7.5 U of DNase (RNase free; Pharmacia) was added and incubation at 37°C was continued for 30 min. Thereafter, the reaction mixture was passed through a Sephadex G-50 column (31) and further purified by phenol extraction and ethanol purification.

RNA transfection. If not specified, transfection was done with a suspension of 3 × 10^6 MDBK cells and about 300 ng of in vitro-transcribed RNA bound to DEAE-dextran (Pharmacia). For the positive control, 5 μg of total RNA from MDBK cells infected with BVDV Oregon was used. The RNA/DEAE-dextran complex was established by mixing RNA dissolved in 100 μl of Hanks balanced salt solution (HBSS) (38) with 100 μl of DEAE-dextran (1 mg/ml) in HBSS) and incubating the mixture for 30 min on ice (38). Pelleted cells were washed once with DMEM without FCS, centrifuged, and then resuspended in the RNA/DEAE-dextran mixture. After a 30-min incubation at 37°C, 20 μl of dimethyl sulfoxide was added and the mixture was incubated for 2 min at room temperature. After addition of 2 ml of HBSS, the cells were pelleted and washed once with HBSS and once with medium without FCS. The cells were resuspended in DMEM with FCS and seeded. If not specified, the cells were initially seeded in a 10-cm-diameter dish and split 48 h to 72 h posttransfection as appropriate for subsequent analyses. For determination of transfection efficiency, the cells were seeded after transfection in three tissue culture dishes 3.5 cm in diameter and peroxidase-stained plaques were counted 2 days posttransfection.

Northern (RNA) hybridization. RNA preparation, gel electrophoresis, radioactive labelling of the probe, hybridization, and posthybridization washes were done as described previously (29). The insert of the BVDV cDNA clone NCII.1 (19) was used as a probe.

Radioimmunoprecipitation and SDS-PAGE. Extracts of MDBK cells transfected with RNA transcribed from the respective infectious cDNA clones and radiolabeled with 0.25 mCi of [^{35}S]methionine-[^{35}S]cysteine ([^{35}S]TransLabel;

ICN) were prepared as described previously (16). For the formation of precipitates, cross-linked *Staphylococcus aureus* was used (15). Sodium dodecyl sulfate-polyacrylamide gel electrophoresis (SDS-PAGE) of proteins was carried out on gels by the method of Doucet and Trifaro (10). The gels were processed for fluorography by using En³Hance (New England Nuclear, Boston, Mass.). For precipitation, an antiserum against NS3 (anti-A3: raised against a bacterial fusion protein encompassing sequences of CSFV Alfort Tübingen) was used (36). NS2-3 cleavage efficiencies were determined based on transient expression with the T7 vaccinia virus system as described previously (16). For evaluation of cleavage efficiencies, the number of methionines and cysteines within NS2-3 or NS3 was determined. After measurement of the radioactivity of the NS2-3 protein with a Fujifilm BAS-1500 phosphorimager (Raytest, Straubenhardt, Germany) (16), the percentage of the counts resulting from the NS3 moiety was calculated. This value, together with the counts determined for the cleaved NS3 protein, was defined as total NS3 (100%). The calculated percentage of cleaved NS3 with respect to total NS3 is given as the percent cleavage efficiency.

RESULTS

Establishment and analysis of an infectious cDNA clone for BVDV Oregon. To investigate the relationship between the efficiency of NS2-3 cleavage and the cytopathogenicity of BVDV Oregon, an infectious cDNA clone of this virus was needed. Within the genus *Pestivirus*, generation of recombinant viruses has been reported for three CSFV isolates as well as for two BVDV strains (18, 21, 22, 24, 39). By analogy to these constructs, the BVDV Oregon clone was designed for runoff transcription of a genome-like RNA with a bacteriophage RNA polymerase. As a basis for construction, the infectious cDNA clone pA/BVDV, which is derived from the BVDV CP7 genome, was used (22).

Pestivirus sequences contain a conserved *Xho*I site at about position 200 as well as a conserved *Aat*II site about 50 nucleotides upstream of the 3′ end. Therefore, the *Xho*I-*Aat*II fragment of pA/BVDV could be exchanged for the sequence of BVDV Oregon. Because of an internal recognition sequence, the *Sma*I site used for linearization of pA/BVDV prior to in vitro transcription (22) was not appropriate for the Oregon clone and was therefore changed into an *Srf*I site, which was also used for other infectious pestivirus cDNA clones (21, 24, 28). The variant of pA/BVDV with the *Srf*I site was termed pC7 and served as basis for the exchange of the *Xho*I-*Aat*II fragment with the BVDV Oregon sequence.

Analysis of the BVDV Oregon genome by cDNA cloning and sequencing has been described in a previous paper (16).

This sequence corresponds to nucleotides (nt) 16 to 12205 and contains the *Xho*I site but not the desired *Aat*II site. To obtain a 3′-terminal cDNA fragment encompassing the *Aat*II site, RT-PCR was performed. The different cDNA clones of BVDV Oregon were fused at appropriate restriction sites by standard procedures. Upstream of the 5′ end of the pestiviral sequence, a T7 RNA polymerase promoter for in vitro transcription was inserted. The resulting full-length cDNA clone coding for the complete polyprotein of BVDV Oregon was termed pOR. The sequence arrangement at the ends of the viral sequence allows the transcription of an RNA without nonviral terminal residues (Fig. 1).

Runoff RNA transcripts synthesized with phage T7 RNA polymerase from *Srf*I-linearized pOR were transfected into MDBK cells. RNA derived from pOR linearized with *Apa*I leading to a 3′-terminal truncation served as a control. Since BVDV Oregon represents a cp virus, recovery of infectious viruses after RNA transfection should result in detection of plaques. Indeed, transfection of full-length RNA derived from pOR led to cell lysis, which could not be observed after transfection of the 3′-terminally truncated RNA. In addition, BVDV-specific RNA could be detected by Northern blot analysis after transfection of the full-length RNA, in contrast to transfection of the truncated RNA (data not shown).

To obtain a virus with a genetic tag that could be easily demonstrated, a second version of the clone was established containing a silent *Xho*I site at nt 5126 to 5131 (pOR/XhoI) (the nucleotide position refers to the sequence published for BVDV SD1 [8]). Transfection of RNA transcribed in vitro from the *Srf*I-linearized plasmid pOR/XhoI resulted in detection of a cytopathic effect (CPE) and of BVDV-specific RNA by Northern blot analysis. In a PCR-based assay, the presence of the *Xho*I site could be shown after passage of the recovered virus (data not shown). These data demonstrated that RNA transcribed from pOR is able to induce the generation of infectious BVDV upon transfection into appropriate cells.

The specific infectivity of the in vitro-transcribed RNA was determined after transfection of different amounts of this RNA or of total RNA from cells infected with BVDV Oregon. On the average, the RNA transcribed in vitro from pOR yielded 8.1×10^3 PFU/µg. The specific infectivity of wild-type RNA
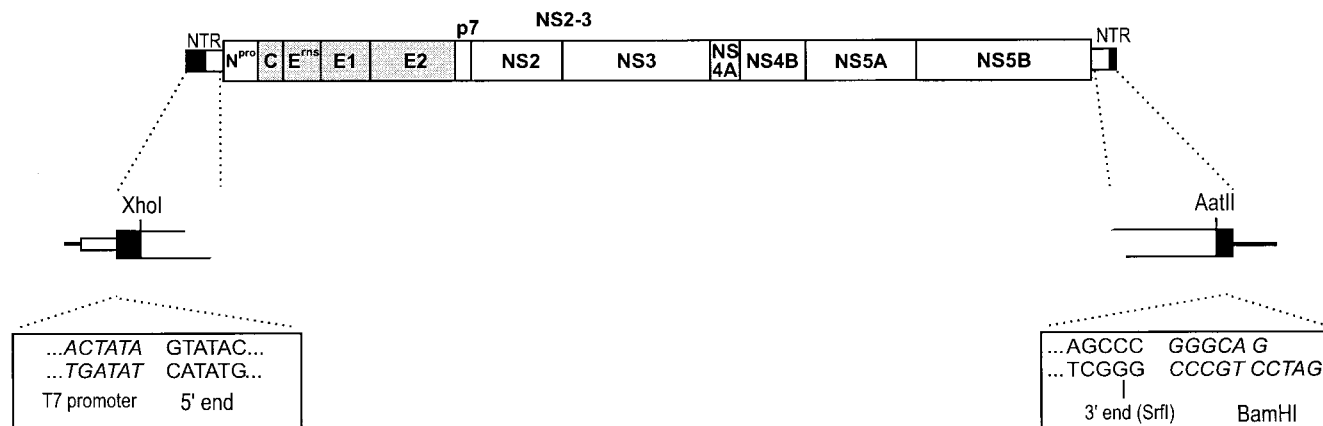

FIG. 1. Schematic presentation of the BVDV full-length cDNA clone pOR. The part of the plasmid containing the complete cDNA derived from the BVDV Oregon genome is shown. The upper part indicates the cDNA, with thin bars at the ends representing the nontranslated regions (NTR) and the thick bar in the middle corresponding to the open reading frame coding for the viral proteins, which are also indicated. Solid bars represent the heterologous sequences derived from pA/BVDV, the infectious clone of BVDV CP7 (22). Gray boxes represent the regions coding for the structural proteins, whereas open boxes are indicative of sequences encoding nonstructural proteins. Below the scheme of the genome, blowups of the nontranslated regions and flanking regions containing the T7 RNA polymerase promoter (thin white box) and the *Srf*I site necessary for runoff transcription are shown. Thin black lines represent plasmid sequences. The *Xho*I site is located at nt 224 to 229, whereas the *Aat*II site represents nt 12268 to 12273 (numbers refer to BVDV SD1 [8]).
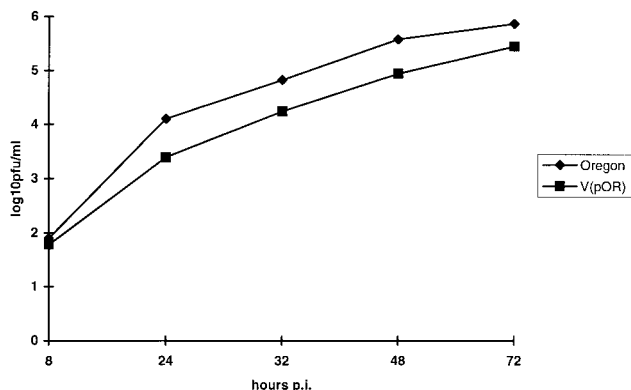
FIG. 2. Growth curve of BVDV Oregon and the virus derived from construct pOR [V(pOR)]. Cells were infected with the viruses at an MOI of 0.02 and harvested by freezing and thawing at the indicated time points. Titers were determined after infection of new cells by counting the number of plaques 72 h postinfection (p.i.) The results are given as $\log_{10}$ PFU per milliliter.

was 9.5×10^3 PFU/μg as determined after transfection of total RNA from cells infected with BVDV Oregon. The amount of viral RNA contained in the sample was determined after Northern blot hybridization by comparison with defined amounts of in vitro-transcribed RNA by using a phosphorimager.

To analyze the growth characteristics of the recombinant virus V(pOR), the transfected cells were harvested by freezing and thawing, and the recovered virus was passaged once. The virus stock thus obtained and wild-type BVDV Oregon were used to infect cells at a MOI of 0.02. At different time points postinfection, cell extracts were prepared from individual dishes by freezing and thawing, and the amount of infectious virus within each culture was determined. While BVDV Oregon reached a titer of 7.4×10^5 PFU/ml at 72 h p.i., the titer of V(pOR) was determined to be 2.8×10^5 PFU/ml (Fig. 2). A slight difference in the titers of the two viruses was also observed at the other time points. However, the difference was only small, and the infectious clone pOR seemed suitable for the desired experiments.

Recovery and analysis of viruses with heterologous NS2 genes. Previous studies revealed that a set of point mutations within NS2 of BVDV Oregon is responsible for NS2-3 processing (16). This was shown by transient expression of chimeric constructs containing cDNA fragments derived from BVDV Oregon and a noncp BVDV. To analyze the correlation between NS2-3 processing and cytopathogenicity, chimeric full-length BVDV cDNA clones were constructed. It was already shown for BVDV CP7 that the presence of the CP7-specific insertion of 27 nt within the NS2 gene is responsible for NS2-3 cleavage; the deletion of this insertion from an infectious cDNA clone of BVDV CP7 led to the recovery of a noncp virus (22, 35). After exchanging the NS2 gene of the full-length cDNA clone pOR for the corresponding sequence of this recombinant noncp virus [here termed V(pC7$_{NS2/}$ $_{C7Ins-}$)], a chimeric virus [V(pOR$_{NS2/C7Ins-}$)] could be recovered as shown by the staining with BVDV-specific antibodies (Fig. 3A). Since V(pOR$_{NS2/C7Ins-}$) showed a noncp phenotype (Fig. 3B), an essential part of the genetic information necessary for cytopathogenicity has to be localized within NS2 of BVDV Oregon. However, the NS2 gene of a heterologous cp BVDV is also able to confer a cp phenotype to BVDV Oregon. This was demonstrated by the recovery of the chimeric cp virus V(pOR$_{NS2/C7}$) after exchange of the NS2 gene of BVDV Oregon for the NS2 gene of the cp strain CP7 (Fig. 3A and B).
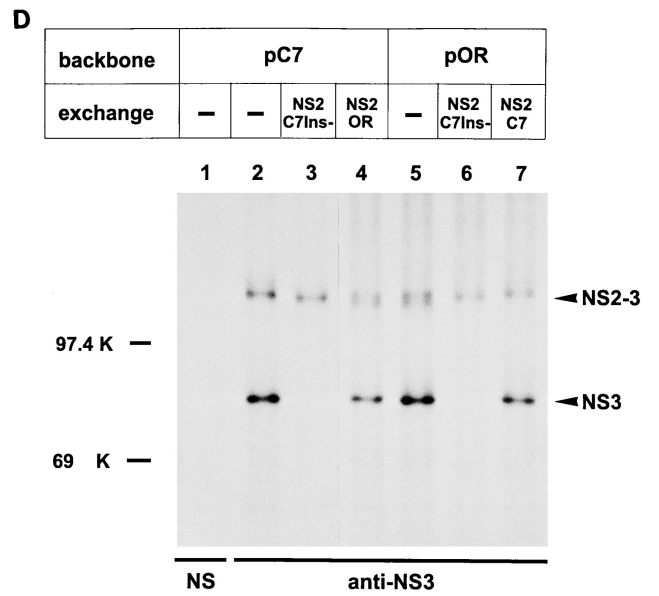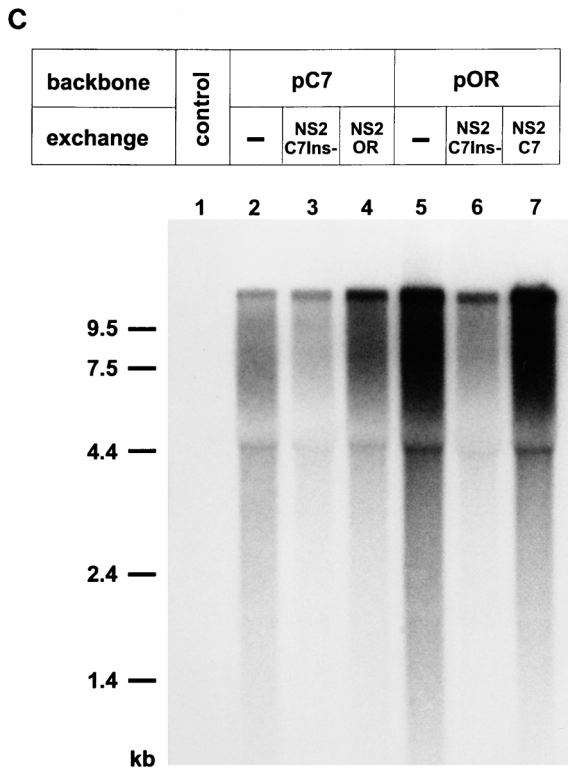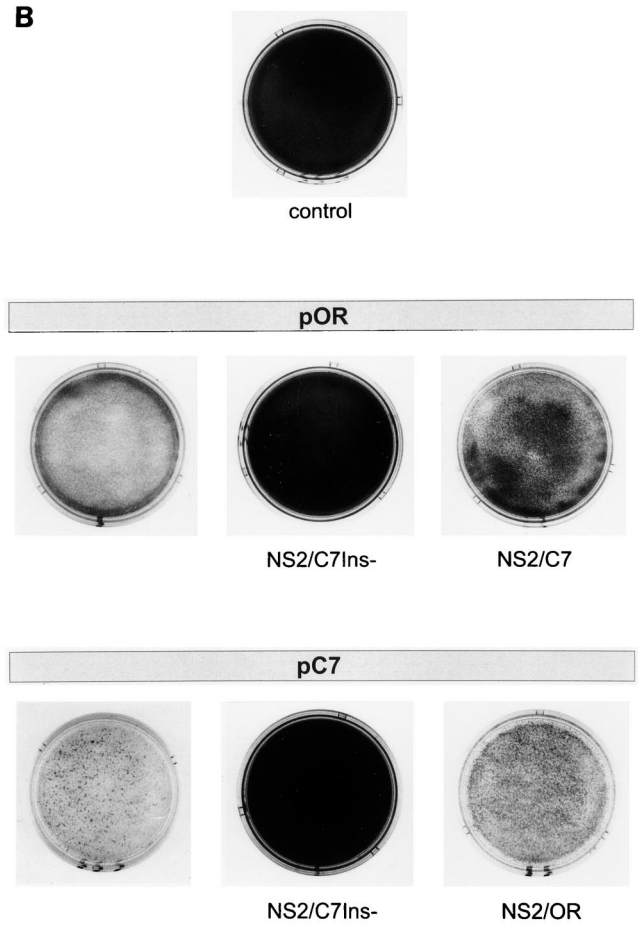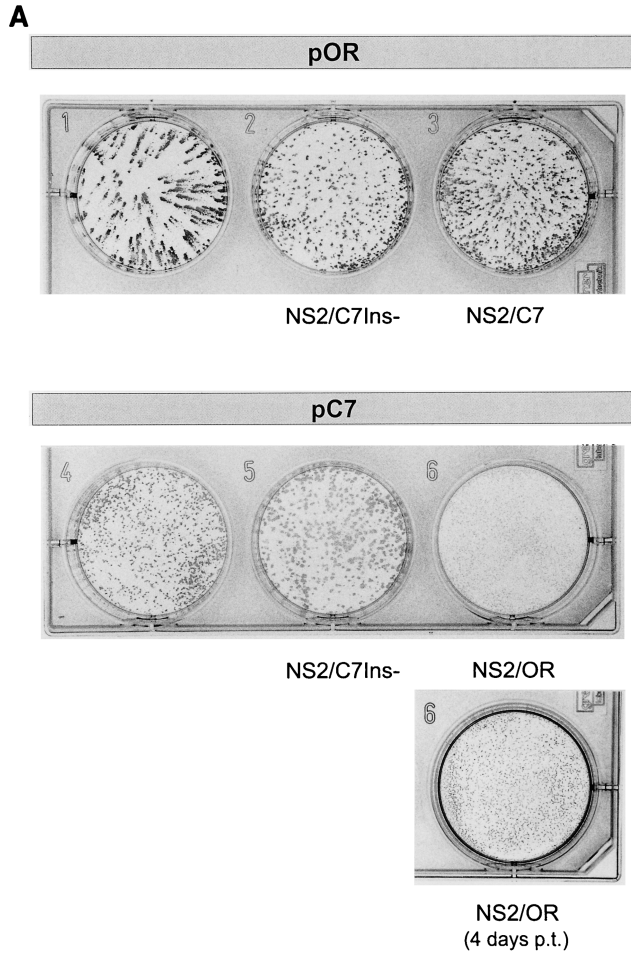
To analyze whether the NS2 gene of BVDV Oregon is sufficient for induction of a cp phenotype, the NS2-coding part of the BVDV Oregon sequence was inserted into the backbone of pC7. The recovered virus [V(pC7$_{NS2/OR}$)] grew very slowly (Fig. 3A) but nevertheless was able to induce clearly detectable CPE (Fig. 3B). Analysis of the RNA of transfected cells in a Northern blot revealed the presence of BVDV RNA for all the chimeras (Fig. 3C).

The correlation between cytopathogenicity and NS2-3 cleavage was investigated after transfection of MDBK cells with the different recombinant viruses and protein labeling with [^{35}S]Met-[^{35}S]Cys. Immunoprecipitation with an antiserum directed against a part of NS3 revealed that both NS3 and NS2-3 could be detected for the recombinant cp viruses whereas only NS2-3 could be precipitated from cells infected with the recombinant noncp viruses (Fig. 3D).

The size of the foci observed after peroxidase staining 72 h posttransfection already indicated differences in the growth characteristics of the recombinant viruses (Fig. 3A). In particular, V(pC7$_{NS2/OR}$), the virus containing the NS2 gene of BVDV Oregon in the context of the CP7 genome, spread very slowly. To analyze the production of infectious progeny virus, growth curves were recorded. After passage and preparation of cell extracts, sufficient titers of the recombinant viruses were obtained to allow infection of cells at an MOI of 0.02. The amount of infectious virus present at different time points was determined by titer measurement on MDBK cells (Fig. 3E). All the chimeric viruses showed growth retardation compared to the wild-type viruses. Particularly pronounced reductions in growth rates were observed for V(pOR$_{NS2/C7Ins-}$) and V(pC7$_{NS2/OR}$). For the latter recombinant, the analysis of focus size showed reduced spread, whereas the noncp chimera based on BVDV Oregon was not found to be considerably impaired in the focus assay.

Experiments with full-length cDNA clones containing single-point mutations in the NS2 gene. Our previous analyses had revealed that the exchange of a single amino acid within NS2 of BVDV Oregon can reduce NS2-3 cleavage. Most striking was an exchange of codon 1555 of the long open reading frame. The BVDV Oregon sequence codes for an S at this position, whereas the genomes of other BVDV strains contain an F codon. Changing S to F in the BVDV Oregon sequence led to reduction of NS2-3 cleavage efficiency to 50% of the wild-type level (16). To analyze the effect of this single-site exchange on the viability and cytopathogenicity of BVDV Oregon, a mutant full-length construct was established. RNA derived from pOR bearing an F codon instead of the S codon at position 1555 (pOR/S-F) led to foci 3 days after RNA transfection, as visualized by MAb-mediated peroxidase staining (Fig. 4A). Compared to RNA derived from the full-length cDNA clone pOR, the specific infectivity was in the same range, as could be seen from the number of foci detectable 3 days after transfection, but the size of plaques was markedly reduced (Fig. 4A). Moreover, a CPE was visible 3 days after transfection of RNA derived from pOR, whereas cp plaques could not be detected at this time point for RNA transcribed from pOR/S-F. However, single cp plaques were seen in the latter case after the cells were split twice at intervals of 3 to 4 days; at this time, nearly all the cells proved to be infected in an immunofluorescence assay (not shown). Splitting the cells again two more times resulted in a severe CPE. However, RT-PCR (primers BVD56 and BVD57) conducted with total RNA derived from such cells showed reversion of the F codon to an S codon.

To analyze the course of the reversion in more detail, RNA transfection was repeated and RNA was isolated from the

A

B

C

backbone	control	pC7			pOR		
exchange		—	NS2 C7Ins-	NS2 OR	—	NS2 C7Ins-	NS2 C7
	1	2	3	4	5	6	7

9.5 —
7.5 —
4.4 —
2.4 —
1.4 —

kb

D

backbone	pC7				pOR		
exchange	—	—	NS2 C7Ins-	NS2 OR	—	NS2 C7Ins-	NS2 C7
	1	2	3	4	5	6	7

97.4 K —

69 K —

◄ NS2-3

◄ NS3

NS   anti-NS3

E

transfected cells at different time points. RT-PCR followed by nucleotide sequencing showed that immediately after transfection as well as after one passage of the transfected cells, all the viral genomes seemed to contain the mutation. However, after the second passage, part of the population had reverted, and after the third passage, the majority of the genomes showed reversion (Fig. 4B). At this time point, plaques showing CPE were detected for the first time. The experiment was repeated three more times. Again, the first cp plaques became visible after the third passage, and analysis of the codon present at position 1555 after the fifth passage revealed reversion to an S codon (data not shown). Within the limits of the experimental system, reversion was complete after five passages and occurred at least predominantly to the wild-type sequence.

The importance of the amino acid at position 1555 for NS2-3 cleavage was demonstrated before also with an approach based on the CP7Ins− sequence. Substitution of the F present at this position of the respective sequence for an S resulted in a change of NS2-3 cleavage efficiency from 0 to 8% (16). When the F codon at position 1555 was exchanged for an S codon in the infectious clone pC7Ins−, no infectious virus could be recovered after RNA transfection. Only single positive cells were detectable when performing immunofluorescence assays 3 days after RNA transfection, and passaging of the transfected cells did not result in recovery of infectious virus (data not shown). Thus, position 1555 seems to be important for both NS2-3 cleavage and viability of the mutant viruses.

Effects of random changes at position 1555. In the next set of experiments, we analyzed the effects of other amino acid exchanges at position 1555 of the BVDV Oregon polyprotein. The NS2-3 cleavage efficiencies of the mutated polyproteins containing the respective exchanges were determined in the T7 vaccinia virus system as described in a previous paper (16). A change of the S to C, an amino acid with similar size and polarity, resulted in the detection of efficient NS2-3 cleavage (78% [Table 1]). After transfection of the RNA derived from the full-length cDNA clone bearing this mutation, large plaques were detectable (Fig. 5). The same was true for the change to T, which also represents a polar amino acid and led to a cleavage efficiency of 70% (Fig. 5). Similar results could be obtained after introduction of A or G at the respective position (Fig. 5), indicating that a polar character of the amino acid at position 1555 is not necessary for efficient NS2-3 cleavage and growth of the virus. Interestingly, the exchange of S for P, which may be supposed to have major effects on the structure of the protein, resulted in efficient NS2-3 processing and a strongly growing virus (Fig. 5). For the change to R, a large but
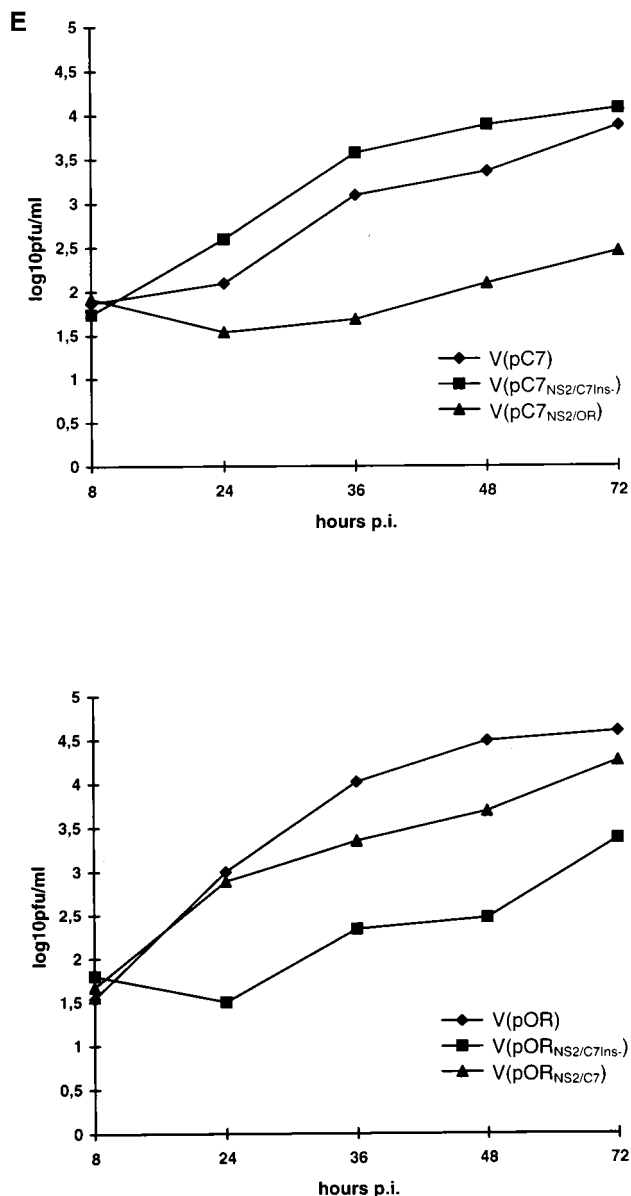
FIG. 3. Analysis of transfection experiments carried out with RNA transcribed from the parental plasmids pOR and pC7, as well as the chimeric plasmids pOR$_{NS2/C7Ins-}$, pOR$_{NS2/C7}$, pC7$_{NS2/C7Ins-}$, and pC7$_{NS2/OR}$. (A) Detection of cells containing replicating virus resulting from RNA transfection. The rows with three dishes show the result of transfection of RNA derived from different full-length constructs based on pOR (upper row) or pC7 (lower row) at 3 days posttransfection. The exchanges present in the constructs are indicated below the dishes. For pC7$_{NS2/OR}$, a second dish is shown that was fixed 4 days posttransfection (p.t.). Cells were transfected with equal doses of the in vitro-transcribed RNAs by using the DEAE-dextran method and seeded at a sufficient density that 3 days posttransfection a closed layer of cells was obtained. At this time point, cells were fixed and virus-containing cells were visualized by MAb-mediated peroxidase staining. By this means, the ability of the mutants to spread can be judged by the size of the foci. (B) Crystal violet staining of tissue culture cells transfected with RNA transcribed from the indicated plasmids. The arrangement of the dishes is similar to that in panel A. An in vitro-transcribed RNA derived from the *Apa*I-linearized plasmid pOR which results in a 3′ terminally truncated BVDV genome served as a negative control. Cells were seeded after transfection and split 3 days later. For pC7, crystal violet staining was done 48 h after the first split. The other cells were split again 96 h after the first split. These cells were stained 48 h (pOR, pC7$_{NS2/OR}$) or 72 h (pOR$_{NS2/}$ $_{C7Ins-}$, pOR$_{NS2/C7}$, pC7$_{NS2/C7Ins-}$, and control) after the second split. (C) Northern blot with RNA isolated from the transfected cells. The cells were split 72 h posttransfection, and RNA was prepared 48 h after the split. For the noncp viruses, 5 μg of total RNA of the transfected cells was loaded on the gel, whereas

for the cp viruses, only 2 μg of RNA was loaded. Hybridization was performed with a BVDV-specific probe. The panel above the gel describes the plasmids from which the different viruses were derived. Interestingly, the recombinant cp viruses seem to produce more viral RNA than the corresponding noncp viruses. Similar results were obtained for a recombinant pair of cp and noncp BVDV obtained from an infectious cDNA clone based on strain NADL (18). (D) SDS-Page analysis of immunoprecipitates after transfection of MDBK cells with RNA derived from the indicated plasmids. Cells were split 72 h posttransfection and labeled with [^{35}S]methionine-[^{35}S]cysteine for 14 h starting either soon after the split (pC7) or 48 h later (pOR, pOR$_{NS2/C7Ins-}$, pOR$_{NS2/C7}$, pC7$_{NS2/C7Ins-}$, and pC7$_{NS2/OR}$). Above the gel, the parental full-length clones are indicated; below this is shown the origin of the NS2 gene for the chimeric viruses (the dashes indicate no exchange of sequences). Precipitation was carried out with an anti-NS3 serum (36), which recognizes NS2-3 and NS3, or with a rabbit preimmune serum (NS). (E) Growth curve of the recombinant viruses with heterologous NS2 genes. Cells were infected with the viruses at an MOI of 0.02 and harvested by freezing and thawing at the indicated time points. Titers were determined after infection of new cells by counting the number of plaques 72 h postinfection (p.i.). The results are given as log$_{10}$ PFU per milliliter.

A

S
88%

S→F
44%

B

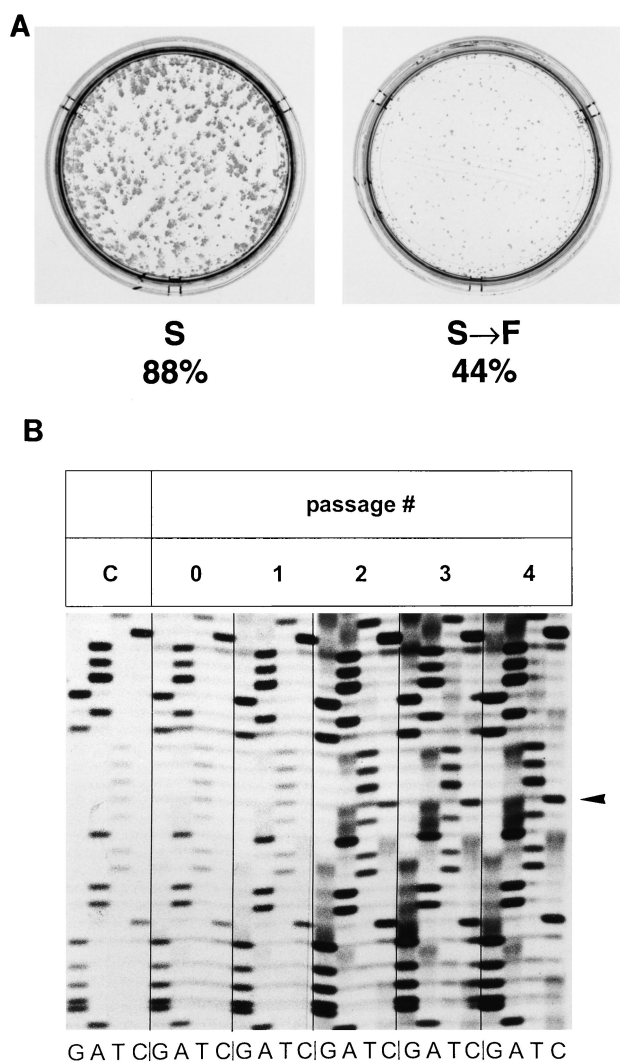G A T C | G A T C | G A T C | G A T C | G A T C | G A T C

FIG. 4. Analyses following the transfection of RNA derived from pOR with the S codon at position 1555 of the ORF exchanged for an F codon. (A) Detection of cells containing replicating virus resulting from RNA transfection. Cells were transfected with equal doses of the in vitro-transcribed RNAs by the DEAE-dextran method and seeded at a sufficient density that 3 days posttransfection a closed layer of cells was obtained. At this time point, cells were fixed and virus-containing cells were visualized by MAb-mediated peroxidase staining. Below the dishes, the NS2-3 cleavage efficiency determined for the respective polyprotein after transient expression is indicated. (B) Analysis of part of the NS2 sequence from RNA obtained at different time points after transfection of RNA derived from pOR/S-F. Cells were split every 3 to 4 days after transfection, and total RNA was prepared from each passage and used as starting material for RT-PCR. RNA from passage 0 was isolated 3 days posttransfection. The amplified fragments were directly sequenced to look for the mutation introduced into pOR/S-F (arrowhead). In lanes C, the sequence of the RT-PCR product derived from the in vitro-transcribed RNA is shown as a control.

charged amino acid, NS2-3 cleavage was 61%, and in comparison to the previously shown mutants, spread of the respective virus was slightly reduced (Fig. 5).

In contrast to the S-to-A mutant, the V mutant grew much less strongly, as could be seen by the small plaques; NS2-3 cleavage was decreased for this mutant (48% [Fig. 5]). Even lower NS2-3 cleavage efficiencies were observed for the Y, L, and D mutants (27, 24, and 18% [Table 1]), and again the respective mutant viruses had smaller plaques, showing that low NS2-3 cleavage efficiencies correlate with reduced rates of

virus growth (Fig. 5). These data also indicate that the mutant viruses reach growth rates similar to the wild-type level only when NS2-3 cleavage efficiency is above 61%.

While a CPE was detectable about 3 days after transfection for the wild-type recombinant virus and the mutants bearing a C, A, or G at position 1555, the CPE developed slightly later for the P, T, and R mutants, probably due to the lower NS2-3 cleavage efficiency and/or the growth retardation. When analyzing the position of the genome coding for aa 1555 after five passages, no revertants could be identified for these mutants (Table 1). With regard to cytopathogenicity, the viruses expressing NS2-3 with V, Y, or L at position 1555 behaved like the F mutant. For these viruses, single cp plaques could first be detected after three passages. In contrast, the D mutant had already developed single cp plaques after the first passage (data not shown). It was striking that the appearance of the first cp plaques always correlated with the detection of revertants or pseudorevertants, as determined by sequencing (data not shown). The term "pseudorevertants" is used here to indicate mutations that affect the same codon (codon 1555) but do not result in the wild-type sequence. The codons obtained for the respective pseudorevertants are listed in Table 1. In all cases, the mutation leads to a sequence coding for an amino acid for which efficient NS2-3 cleavage was observed before. Northern blot analysis of total RNA from the cells of the fifth passage showed the absence of defective interfering particles (data not shown), indicating that the CPE is due to the original mutants, revertants, or pseudorevertants, respectively.

To obtain a mutant for which the probability of reversion is lower, we decided to delete the S at position 1555 within the sequence of BVDV Oregon. Interestingly, after expression of the respective mutant polyprotein with the T7 vaccinia virus system, a cleavage efficiency of 57% was determined (Table 1). Even more surprisingly, infectious virus could be recovered from the infectious full-length cDNA clone of BVDV Oregon containing the deletion (Fig. 5). However, in spite of the relatively high cleavage efficiency, the recovered virus showed small foci after peroxidase staining 3 days posttransfection and no CPE was detectable. It was not possible to decide whether a CPE appeared after five passages, since no cp plaques were visible; only some more dead cells in the supernatant were observed. However, when the cells of the fifth passage were harvested by freezing and thawing and the lysate was used for reinfection of fresh cells, plaques were visible. To analyze the NS2 sequence of the virus obtained after five passages, the NS2 gene was amplified by RT-PCR with primers M1 (16) and BVDV 57 and sequenced directly. Sequence analysis of the obtained product revealed that the deletion was still present and that no second-site mutations were detectable within NS2.

DISCUSSION

Cytopathogenic isolates of BVDV express the nonstructural protein NS3, which is not found in cells infected with noncp BVDV and therefore represents the marker protein of cp BVDV. Elaborate studies with different BVDV strains revealed that expression of NS3 is caused by genome alterations resulting from RNA recombination (20). Recently, we determined for the cp BVDV Oregon a new mechanism of NS3 expression that is not due to RNA recombination but is based on point mutations within NS2 (16). To give final proof that these point mutations not only are responsible for NS2-3 cleavage but also cause the cytopathogenicity of the respective virus, analyses involving site-directed mutagenesis of the viral genome had to be performed with an infectious clone for BVDV Oregon. Approximately the first 200 and last 50 nt of the viral

TABLE 1. Effects of mutations of the codon at position 1555 of the ORF in the full-length clone pOR on NS2-3 cleavage efficiency and stability of the mutations after five passages

Amino acid (codon) at position 1555[a]	NS2-3 cleavage efficiency (%)[b]	Amino acid change at position 1555 after 5 passages[c]
S (TCT)	88	None
A (GCT)	82	None
C (TGT)	78	None
G (GGT)	76	None
P (CCT)	72	None
T (ACT)	70	None
R (CGT)	61	None
V (GTT)	48	A (GCT)
F (TTT)	44	S (TCT)
Y (TAT)	27	C (TGT)
L (CTT)	24	P (CCT)
D (GAT)	18	G (GGT)/A (GCT)
ΔS	57	None

[a] Amino acids at position 1555 of the polyprotein encoded by BVDV Oregon or the different mutants based on pOR. Serine represents the amino acid of the wild-type sequence. In parentheses, the triplets encoding the respective amino acids are indicated, with the exchanged nucleotide(s) underlined.

[b] Efficiency of NS2-3 cleavage determined after transient expression in the T7 vaccina virus system as an average of at least two independent experiments determined as described previously (16).

[c] The analysis of the sequence coding for the amino acid position 1555 after five passages was performed for three independent transfection experiments. For the V, F, Y, and L mutants, the same revertants or pseudorevertans were obtained in each of the three experiments, whereas for the D mutant, alteration to A occurred in two cases and mutation to G occurred in one experiment. In cases in which the introduced mutation was found changed after five passages, the codons are given with the altered nucleotide written in bold type.
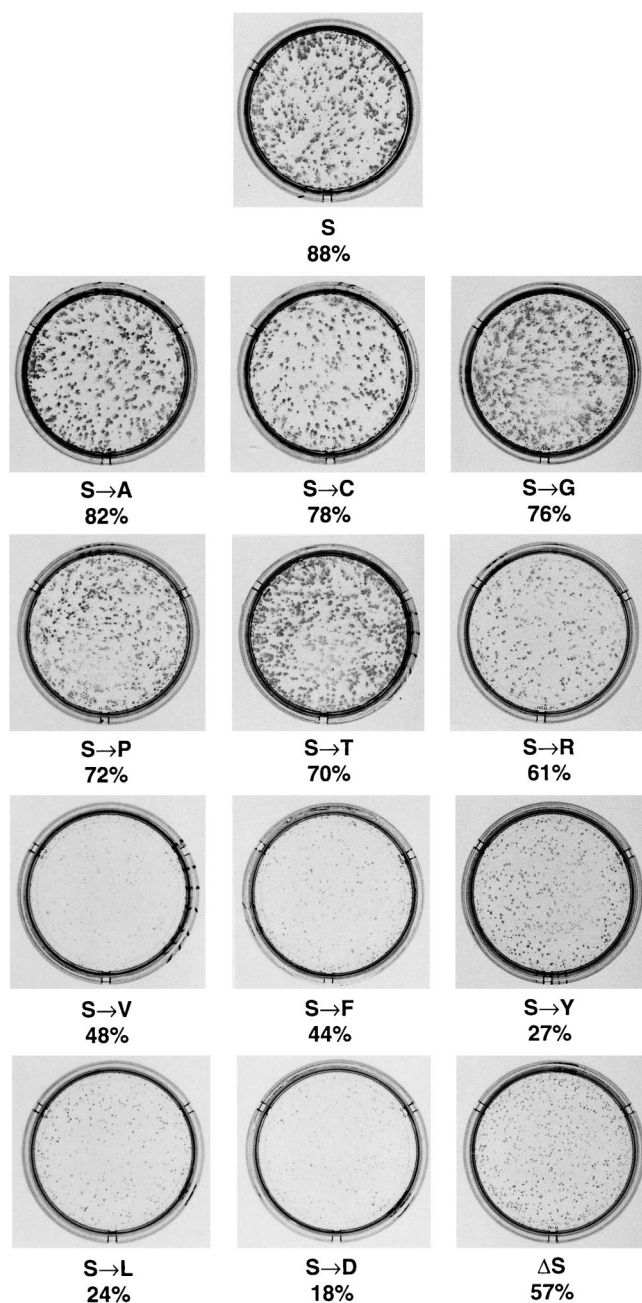

FIG. 5. Analysis of transfection experiments carried out with RNA transcribed from plasmid pOR encoding the wild-type serine at position 1555, or plasmids where the codon at position 1555 had been changed, leading to the point mutation indicated below each dish. In addition, the NS2-3 cleavage efficiency of each mutated polyprotein is given. Cells containing replicating virus were detected 3 days posttransfection as described in the legend to Fig. 4A.

sequence in our full-length construct pOR were derived from the infectious cDNA clone of BVDV CP7 (pA/BVDV) (22). The specific infectivity of the RNA transcribed from pOR is in the same range as that of the viral RNA. Also with regard to the growth rates, only small differences were observed between the recovered virus and wild-type virus. Similar reductions in growth rates were also observed for some other recombinant pestiviruses (21, 22). It therefore can be concluded that the sequences derived from pA/BVDV are compatible with the

Oregon sequences, although many exchanges and also small insertions are present in pOR with regard to the BVDV Oregon genome in a region that can be supposed to be of functional relevance for RNA replication and moreover is part of the internal ribosome entry site (IRES) responsible for initiation of translation (25, 27).

In a previous paper, we showed by transient-expression studies that NS2 of BVDV Oregon in the context of the sequence of a noncp BVDV leads to NS3 expression (16). The experiments described in the present paper demonstrate that the presence of the NS2 gene of BVDV Oregon in a heterologous infectious clone is sufficient for the recovery of a cp virus from the transcribed chimeric RNA. Also, after exchanging the NS2 gene within the genome of BVDV Oregon with the respective sequence derived from a noncp virus, a noncp virus was recovered. These conclusions could be drawn even though the recombinant viruses showed differences with regard to focus morphology, virus spread, and efficiency of generating infectious progeny viruses. In particular, some of the chimeric viruses were severely hampered. Differences were also observed in the time needed by the cp viruses for development of severe CPE. However, the earliest cp plaques could be consistently detected for all the cp viruses 72 h posttransfection, indicating that identification of CPE in our system is not dependent on efficient virus growth. Since the NS2 proteins expressed by the chimeric viruses are functional in the parental viruses, the reduced viability of some of the chimeric viruses is most probably due to problems in the interaction of the foreign NS2 with, e.g., some other viral protein(s). In future experiments, we will try to generate pseudorevertants of these viruses in passage experiments to identify putative partners interacting with NS2 and thus learn more about the possible functions of this interesting protein.

Protein studies of the recombinant viruses containing the heterologous NS2 genes confirmed that cytopathogenicity correlates with NS3 expression. It therefore can be concluded that the NS2 gene of BVDV Oregon indeed contains all the information necessary for a cp phenotype and that, as already observed in experiments with other infectious BVDV clones, expression of NS3 presumably causes the CPE (18, 22). The mechanism by which NS3 might induce cell lysis is still obscure.

So far, BVDV Oregon represents the only pestivirus, for which a method for stepwise modulation of NS2-3 cleavage efficiency has been established. To analyze whether the rate of NS2-3 cleavage correlates with the intensity of the CPE and whether a kind of threshold value of NS3 expression has to be reached in order to detect cell lysis, we performed a set of experiments with different mutant full-length constructs. The basis for this question was the observation that other pestiviruses, namely, CSFV and some border disease viruses, express NS3 without being cytopathogenic (2, 36). The reason for this has still to be elucidated. Protein analyses showed that these viruses express less NS3 than cp BVD viruses (2, 36). This observation led to the hypothesis that in these cases the amount of NS3 might not be sufficient for induction of cell lysis. According to our previous studies, the efficiency of NS2-3 cleavage varied considerably for BVDV Oregon after expression of proteins containing single point mutations within NS2 (16). The change of S at position 1555 of the polyprotein to F, as well as to V, Y, L, or D, reduced NS2-3 cleavage to 48% of the wild-type level or below. Nevertheless, infectious virus could be obtained after transfection of RNA derived from the respective mutant cDNA clones. However, compared to wild-type BVDV Oregon, these mutants showed small foci after peroxidase staining whereas mutants for which efficient NS2-3 cleavage was determined (C, A, G, P, and T) spread as well as wild-type BVDV Oregon did. The R mutant exhibited slightly reduced rates of NS2-3 cleavage and also a small reduction in foci size.

In contrast to the C, A, G, P, T, and R mutants, which displayed NS2-3 cleavage efficiencies above 60% and remained stable for five passages, reversion could be observed for the F, V, Y, L, and D mutants, indicating a considerable effect of these mutations on virus viability with a significant pressure for selection of mutants not showing this disadvantage. Thus, NS2 plays an essential role in the life cycle of a pestivirus. Recent studies showed that a subgenomic pestivirus RNA replicon which encodes all NS proteins except NS2 and p7, replicates autonomously (3). Accordingly, NS2 is obviously not necessary for basic RNA replication. This finding is in accordance with the data described in the present paper since we observed RNA replication regardless of the mutations within NS2. It is therefore unlikely that the reduction of virus spread observed for some of our mutants is due to a problem concerning basic RNA replication. Nevertheless, an influence on the efficiency of RNA replication could not be excluded, especially since there are indications for enhanced RNA synthesis in cp BVDV that might be due to NS2-3 cleavage (18). We therefore conducted pilot experiments with some of the mutants to determine the influence of the mutations on the level of viral RNA present within cells early after transfection. Indeed, a reduction in the level of intracellular viral RNA was detected in some cases; the lowest values were around 20% of the wild-type level (Meyers, unpublished). In general, we observed a tendency toward reduced RNA production for mutants with lower NS2-3 cleavage efficiencies, but there was no strict correlation between the level of RNA and the cleavage efficiency. As an example, the mutants expressing leucine or valine at position 1555 showed rates of RNA synthesis in the range of 50% of the wild-type level, but similar data were also obtained for mutants showing efficient NS2-3 cleavage (Meyers, unpublished). Further analyses including time course experiments will be necessary to definitely find out the influence of NS2 mutations on RNA replication. For these investigations, replicons are needed to avoid the problem of virus spread during prolonged periods of RNA synthesis, and better standardized RNA transfection procedures will have to be developed to allow the precise determination of transfection efficiencies.

If the reduction in virus spread observed for some of our mutants were due not only to a simple decrease in RNA replication, our results could be interpreted in a way that NS2 plays a role in the process of virus formation. Based on the hydrophobic character of the NS2 protein of pestiviruses and the presumption that the N terminus of NS2 is most probably generated by cellular signal peptidase (35), an integration into membranes similar to HCV NS2 can be assumed. It was demonstrated for HCV that the NS2 polypeptide is integrated into the endoplasmatic reticulum membrane and appears to be associated with the envelope proteins of the virus (33). Perhaps NS2 of both pestiviruses and HCV exhibit similar functions to assist in maturation of virus glycoproteins, virus assembly, or virus release.

Regardless of the different putative functions of NS2 and the possible multiple effects of the mutations we introduced into this protein, it has to be stressed that there is a striking correlation between the ability of the mutant viruses to spread in tissue culture and the efficiency of NS2-3 cleavage. The fact that revertants or pseudorevertants were obtained with sequences coding for A, S, C, P, or G at position 1555 after passaging of the V, F, Y, L, and D mutants is again indicative of the functional importance of this correlation, since in all cases changes that allow efficient NS2-3 processing were selected. Thus, in the context of the BVDV Oregon sequence, efficient NS2-3 cleavage represents a considerable advantage. It seems as if a threshold value existed for NS3 expression with respect to the stability of the introduced point mutation. This value must be somewhere between 48 and 61%, since all mutants that showed a cleavage efficiency of 61% or higher remained stable whereas all mutants for which NS2-3 was cleaved with 48% efficiency or less showed reversion.

The main initial aim of our studies was to analyze the influence of NS2-3 cleavage efficiency on the cytopathogenicity of the respective virus mutants. While cell lysis could be observed 3 to 4 days after transfection for the A, C, G, P, T, and R mutants, CPE was visible for the V, F, Y, L, and D mutants only after the cells were split several times. It is difficult to decide whether the delayed induction of CPE is a problem of the reduced NS3 expression, a consequence of the diminished growth rate of the mutants, or a combination of the two. However, the fact that nearly all cells proved to be infected in an immunofluorescence assay but only single cp plaques were visible at the time point where the first revertants could be detected suggests that the plaques are due to the arising revertants. Moreover, there was no difficulty in identifying CPE for the chimeric virus V(pC7$_{NS2CP7}$) as early as 72 h after RNA transfection, even though this virus was severely impaired with regard to spread and generation of infectious progeny virus. It therefore can be assumed that for BVDV Oregon induction of cell lysis is dependent on the presence of a certain amount of NS3 within the cell, thus connecting the cp phenotype, the ability of the mutants to spread in tissue culture, and the efficiency of NS2-3 cleavage. Again, there seems to be a threshold value somewhere between 48 and 61% of NS2-3 cleavage efficiency that separates noncp and cp viruses. Thus, inefficient cleavage could indeed be the reason why CSFV and certain

border disease virus strains are noncp although they express NS3.

Regarding the importance of the amino acid at position 1555 for efficient NS2-3 cleavage and viability, it was very surprising that deletion of the respective codon from the sequence of BVDV Oregon resulted in a viable virus. The cleavage efficiency for this mutant was found to be 57%; however, a CPE could not be detected after transfection, and it was hard to decide if it developed during passaging. Only when fresh cells were infected with virus from the fifth passage was a CPE observed. The reason for this phenomenon is still obscure. Sequence analyses showed that the deletion was still present after five passages. Moreover, no mutations occurred within the NS2 region. The fact that cleavage also occurs after deletion of S 1555 represents a further argument for the conclusion, that this amino acid does not possess a dominant influence on NS2-3 processing like, e.g., catalytic activity. Our data again support the hypothesis that the conformation of NS2 is important for efficient NS2-3 cleavage and that this conformation may be achieved by different primary sequences. According to this hypothesis, amino acids like C, G, A, T, or P would allow the NS2 protein to fold in a similar way to NS2 bearing S at position 1555, whereas other amino acids like V, F, Y, L, or D would have a major impact on the secondary structure of NS2, resulting in considerably reduced cleavage rates.

Taking all our knowledge of BVDV Oregon, it seems that there is not one but a set of point mutations necessary to cause efficient NS2-3 cleavage. Thus, conversion of a hypothetical noncp precursor to a cp virus like BVDV Oregon would require several changes. This could be achieved by the consecutive accumulation of point mutations, a process supported by the error-prone RNA-dependent RNA polymerases involved in replication of RNA virus genomes. It was therefore surprising that BVDV strains, for which cytopathogenicity is based on point mutations, are obviously much less frequent than those generated by recombination according to a complicated and highly unlikely mechanism. The data obtained during the experiments with the infectious clones can explain this finding. All single exchanges that considerably reduced NS2-3 cleavage efficiencies reverted to better processed sequences. Moreover, we found that some full-length constructs containing chimeric NS2 genes that lead to low efficiency NS2-3 cleavage were not viable at all (data not shown). Similarly, changing the phenylalanine at position 1555 of the CP7Ins− sequence to serine leads to a low level of NS2-3 processing and a nonviable virus (16; B. M. Kümmerer and G. Meyers, unpublished data). Thus, the results of our experiments indicate that with regard to NS2-3 cleavage, two different situations, namely, no processing of the protein at all or cleavage with a certain efficiency, lead to strongly growing BVDV. Accordingly, a BVDV strain would prefer to stay noncp or cp instead of acquiring a hypothetical intermediate phenotype. Thus, a change of the phenotype from noncp to cp by the accumulation of point mutations would be rather unlikely, since it would be necessary to pass through such intermediate stages in which the mutants, if viable at all, would show a strong tendency to revert or pseudorevert in order to allow efficient propagation. As an alternative to accumulation, the appropriate point mutations could be introduced simultaneously, a process that probably is as unlikely as RNA recombination. These considerations could explain why the generation of a cp BVDV strain by point mutations is a rare event and therefore only few cp BVDV strains have been identified so far with point mutations responsible for NS2-3 cleavage and cytopathogenicity. Apparently, the obstacles to the generation of cp BVDV strains like Oregon are equivalent to or even higher than those due to the complicated RNA recombination mechanism.

REFERENCES

1. **Baker, J. C.** 1987. Bovine viral diarrhea virus: a review. J. Am. Vet. Med. Assoc. **1990:**1449–1458.
2. **Becher, P., A. D. Shannon, N. Tautz, and H.-J. Thiel.** 1994. Molecular characterization of border disease virus, a pestivirus from sheep. Virology **198:**542–551.
3. **Behrens, S.-E., C. W. Grassmann, H.-J. Thiel, G. Meyers, and N. Tautz.** 1998. Characterization of an autonomous subgenomic pestivirus RNA replicon. J. Virol. **72:**2364–2372.
4. **Bolin, S. R., A. W. McClurkin, R. C. Cutlip, and M. F. Coria.** 1985. Severe clinical disease induced in cattle persistently infected with noncytopathic bovine viral diarrhea virus by superinfection with cytopathic bovine viral diarrhea virus. Am. J. Vet. Res. **46:**573–576.
5. **Brown, E. A., H. Zhang, L.-H. Ping, and S. M. Lemon.** 1992. Secondary structure of the 5′ nontranslated regions of hepatitis C virus and pestivirus genomic RNAs. Nucleic Acids Res. **20:**5042–5045.
6. **Brownlie, J., M. C. Clarke, and C. J. Howard.** 1984. Experimental production of fatal mucosal disease in cattle. Vet. Rec. **114:**535–536.
7. **De Moerlooze, L., M. Desport, A. Renard, C. Lecomte, J. Brownlie, and J. A. Martial.** 1990. The coding region for the 54-kDa protein of several pestiviruses lacks host insertions but reveals a "zinc finger-like" domain. Virology **177:**812–815.
8. **Deng, R., and K. V. Brock.** 1992. Molecular cloning and nucleotide sequence of a pestivirus genome, noncytopathic bovine viral diarrhea virus strain SD-1. Virology **191:**867–879.
9. **Devereux, J., P. Haeberli, and O. Smithies.** 1984. A comprehensive set of sequence analysis programs for the VAX. Nucleic Acids Res. **12:**387–395.
10. **Doucet, J.-P., and J.-M. Trifaro.** 1988. A discontinuous and highly porous sodium dodecyl sulfate-polyacrylamide slab gel system of high resolution. Anal. Biochem. **168:**265–271.
11. **Fuerst, T. R., E. G. Niles, F. W. Studier, and B. Moss.** 1986. Eukaryotic transient-expression system based on recombinant vaccinia virus that synthesizes bacteriophage T7 RNA polymerase. Proc. Natl. Acad. Sci. USA **83:**8122–8126.
12. **Gillespie, J. H., J. A. Baker, and K. McEntee.** 1960. Cytopathogenic strain of virus diarrhea virus. Cornell Vet. **50:**73–79.
13. **Greiser-Wilke, I., L. Haas, K. Dittmar, B. Liess, and V. Moennig.** 1993. RNA insertions and gene duplications in the nonstructural protein p125 region of pestivirus strains and isolates *in vitro* and *in vivo*. Virology **193:**977–980.
14. **Laude, H.** 1977. Improved method for the purification of hog cholera virus grown in tissue culture. Arch. Virol. **54:**41–51.
15. **Kessler, S. W.** 1981. Use of protein A-bearing staphylococci for the immunoprecipitation and isolation of antigens from cells. Methods Enzymol. **73:**442–459.
16. **Kümmerer, B. M., D. Stoll, and G. Meyers.** 1998. Bovine viral diarrhea strain Oregon: a novel mechanism for processing of NS2-3 based on point mutations. J. Virol. **72:**4127–4138.
17. **Kunkel, T. A., J. D. Roberts, and R. A. Zakour.** 1987. Rapid and efficient site-specific mutagenesis without phenotypic selection. Methods Enzymol. **154:**367–392.
18. **Mendez, E., N. Ruggli, M. S. Collett, and C. M. Rice.** 1998. Infectious bovine viral diarrhea virus (strain NADL) RNA from stable cDNA clones: a cellular insert determines NS3 production and viral cytopathogenicity. J. Virol. **72:**4737–4745.
19. **Meyers, G., N. Tautz, E. J. Dubovi, and H.-J. Thiel.** 1991. Viral cytopathogenicity correlated with integration of ubiquitin-coding sequences. Virology **180:**602–616.
20. **Meyers, G., and H.-J. Thiel.** 1996. Molecular characterization of pestiviruses. Adv. Virus Res. **47:**53–118.
21. **Meyers, G., H.-J. Thiel, and T. Rümenapf.** 1996. Classical swine fever virus: recovery of infectious viruses from cDNA constructs and generation of recombinant cytopathogenic defective interfering particles. J. Virol. **70:**1588–1595.
22. **Meyers, G., N. Tautz, P. Becher, H.-J. Thiel, and B. M. Kümmerer.** 1996. Recovery of cytopathogenic and noncytopathogenic bovine viral diarrhea viruses from cDNA constructs. J. Virol. **70:**8606–8613.
23. **Moennig, V., H.-R. Frey, E. Liebler, J. Pohlenz, and B. Liess.** 1990. Reproduction of mucosal disease with cytopathogenic bovine viral diarrhoea virus selected in vitro. Vet. Rec. **127:**200–203.
24. **Moormann, R. J. M., H. G. P. van Gennip, G. K. W. Miedema, M. M. Hulst, and P. A. van Rijn.** 1996. Infectious RNA transcribed from an engineered

full-length cDNA template of the genome of a pestivirus. J. Virol. **70:**763–770.

25. **Poole, T. L., C. Wang, R. A. Popp, L. N. D. Potgieter, A. Siddiqui, and M. S. Collett.** 1995. Pestivirus translation initiation occurs by internal ribosome entry. Virology **206:**750–754.

26. **Rice, C. M.** 1996. Flaviviridae: the viruses and their replication, p. 931–959. *In* B. N. Fields, D. M. Knipe, and P. M. Howly (ed.), Fields virology, 3rd ed., vol. 1. Lippincott-Raven Publishers, Philadelphia, Pa.

27. **Rijnbrand, R., T. van der Straaten, P. A. van Rijn, W. J. M. Spaan, and P. J. Bredenbeek.** 1997. Internal entry of ribosomes is directed by the 5′ noncoding region of classical swine fever virus and is dependent on the presence of an RNA pseudoknot upstream of the initiation codon. J. Virol. **71:**451–457.

28. **Ruggli, N., J.-D. Tratschin, C. Mittelholzer, and M. A. Hofmann.** 1996. Nucleotide sequence of classical swine fever virus strain Alfort/185 and transcription of infectious RNA from stably cloned full-length cDNA. J. Virol. **70:**3478–3487.

29. **Rümenapf, T., G. Meyers, R. Stark, and H.-J. Thiel.** 1989. Hog cholera virus—characterization of specific antiserum and identification of cDNA clones. Virology **171:**18–27.

30. **Rümenapf, T., R. Stark, M. Heimann, and H.-J. Thiel.** 1998. N-terminal protease of pestiviruses: identification of putative catalytic residues by site-directed mutagenesis. J. Virol. **72:**2544–2547.

31. **Sambrook, J., E. F. Fritsch, and T. Maniatis.** 1989. Molecular cloning: a laboratory manual, 2nd ed. Cold Spring Harbor Laboratory Press, Cold Spring Harbor, N.Y.

32. **Sanger, F., S. Nicklen, and A. R. Coulson.** 1977. DNA sequencing with chain-terminating inhibitors. Proc. Natl. Acad. Sci. USA **74:**5463–5467.

33. **Santolini, E., L. Pacini, C. Fipaldini, G. Migliaccio, and N. La Monica.** 1995. The NS2 protein of hepatitis C virus is a transmembrane polypeptide. J. Virol. **69:**7461–7471.

34. **Stark, R., G. Meyers, T. Rümenapf, and H.-J. Thiel.** 1993. Processing of pestivirus polyprotein: cleavage site between autoprotease and nucleocapsid protein of classical swine fever virus. J. Virol. **67:**7088–7095.

35. **Tautz, N., G. Meyers, R. Stark, E. J. Dubovi, and H.-J. Thiel.** 1996. Cytopathogenicity of a pestivirus correlates with a 27-nucleotide insertion. J. Virol. **70:**7851–7858.

36. **Thiel, H.-J., R. Stark, E. Weiland, T. Rümenapf, and G. Meyers.** 1991. Hog cholera virus: molecular composition of virions from a pestivirus. J. Virol. **65:**4705–4712.

37. **Thiel, H.-J., P. G. W. Plagemann, and V. Moennig.** 1996. Pestiviruses, p. 1059–1073. *In* B. N. Fields, D. M. Knipe, and P. M. Howley (ed.), Fields virology, 3rd ed., vol. 1. Lippincott-Raven Publishers, Philadelphia, Pa.

38. **Van der Werf, S., J. Bradley, E. Wimmer, F. W. Studier, and J. J. Dunn.** 1986. Synthesis of infectious poliovirus RNA by purified T7 RNA polymerase. Proc. Natl. Acad. Sci. USA **83:**2330–2334.

39. **Vassilev, V. B., M. S. Collett, and R. O. Donis.** 1997. Authentic and chimeric full-length genomic cDNA clones of bovine viral diarrhea virus that yield infectious transcripts. J. Virol. **71:**471–478.

40. **Weiland, E., H.-J. Thiel, G. Hess, and F. Weiland.** 1989. Development of monoclonal neutralizing antibodies against bovine viral diarrhea virus after pretreatment of mice with normal bovine cells and cyclophosphamide. J. Virol. Methods **24:**237–244.

41. **Wengler, G., D. W. Bradley, M. S. Collett, F. X. Heinz, R. W. Schlesinger, and J. H. Strauss.** 1995. Flaviviridae, p. 425–427. *In* F. A. Murphy, C. M. Fauquet, D. H. L. Bishop, S. A. Ghabrial, A. W. Jarvis, G. P. Martelli, M. A. Mayo, and M. D. Summers (ed.), Virus taxonomy. Sixth report of the International Committee on Taxonomy of Viruses. Springer-Verlag, Vienna, Austria.